cess has a high run-to-run reproducibility, eliminating the need of expensive equipment for pad surface conditioning and end-point determination. As the removal rate is mainly dependent on the chemical properties of the oxide, high selectivity between different dielectrics and metals can be obtained by the selection of suitable slurries. Another advantage of the process is that high planarization rates are achieved at relatively low slurry concentrations. This combined with increased pad life reduces the cost of consumables, a major consideration in IC manufacturing. A more detailed modeling of the process is needed to further improve the understanding of various factors involved in polishing and their interactions.

Acknowledgments

The authors wish to thank M. B. Ketchen and M. Jaso of IBM for helpful discussions. This work was supported by DoD's University Research Initiative, ONR, BMDO through RADC and initially by ARPA through CSE.

Manuscript submitted Dec. 3, 1994; revised manuscript received May 1, 1995.

State University of New York, Stony Brook, assisted in meeting the publication costs of this article.

REFERENCES

1. L. M. Cook, *J. Non-Crystalline Solids,* **120,** 152 (1990).
2. H. Landis, P. Burke, W. Cote, W. Hill, C. Hoffman, C. Kaanta, C. Koburger, W. Lange, M. Leach, and S. Luce, *Thin Solid Films,* **230,** 1 (1992).
3. W. J. Partrick, W. L. Guthrie, C. L. Standley, and P. M. Schiable, *This Journal,* **138,** 1778 (1991).
4. S. Sivaram, H. Bath, R. Leggert, A. Maury, K. Monnig, and R. Tolles, *Solid State Technol.,* 87 (May 1992.)
5. M. B. Ketchen, D. Pearson, A. W. Kleinsasser, C.-K. Hu, M. Smyth, J. Logan, K. Stawiasz, E. Baran, M. Jaso, T. Ross, K. Petrillo, M. Manny, S. Basavaiah, S. Brodsky, S. B. Kaplan, W. J. Gallagher, and M. Bhushan, *Appl. Phys, Lett.,* **59,** 2609 (1991).
6. F. Preston, *J. Soc. Glass Technol.,* **11,** 214 (1927).
7. S. R. Runnels and L. M. Eyman, *This Journal,* **141,** 1698 (1994).
8. N. J. Brown, P. C. Baker, and R. T. Maney, *SPIE Proc.,* **306,** 42 (1981).
9. T.-K. Yu, C. C. Yu, and M. Orlowski, *IEDM Digest,* p. 865 (1993).
10. R. Jairath, J. Farkas, C. K. Huang, M. Stell, and S.-M. Tzeng, *Solid State Technol.,* 71 (July 1994).
11. R. D. Arnell, P. B. Dacies, J. Halling, and T. L. Whomes, *Tribology Principles and Design Applications,* Chap. 5, pp. 124-160, Springer-Verlag, New York (1991).
12. P. A. Burke, *VMIC,* June 1991, p 379, IEEE, New York (1991).
13. P. Renteln, M. E. Thomas, and J. M. Pierce, *VMIC,* June 1990, p. 57, IEEE, New York (1990).
14. J. Warnock, *This Journal,* **138,** 2398 (1991).
15. S. R. Runnels, *ibid.,* **141,** 1900 (1994).
16. R. Kolenkow and R. Nagahara, *Solid State Technol.,* p. 112 (June 1992).
17. M. Bhushan, R. Rouse, and J. E. Lukens, *VMIC,* June 1994, p 216, IEEE, New York (1994).
18. Z. Bao, M. Bhushan, S. Han, and J. E. Lukens, in *Proceedings of Applied Superconductivity Conference,* Oct. 1994.
19. P. Bunyk, A. Oliva, V. Semenov, M. Bhushan, K. K. Likharev, J. E. Lukens, M. B. Ketchen, and W. H. Mallison, *Appl. Phys. Lett.,* **66,** 646 (1995).

Ceramic Membranes by Electrochemical Vapor Deposition of Zirconia-Yttria-Terbia Layers on Porous Substrates

Hendrik W. Brinkman and Anthonie J. Burggraaf

Laboratory of Inorganic Materials Science, Faculty of Chemical Technology, University of Twente, 7500 AE Enschede, The Netherlands

ABSTRACT

By means of electrochemical vapor deposition (EVD), it is possible to grow thin, dense layers of zirconia/yttria/terbia solid solution (ZYT) on porous ceramic substrates. These layers can be used as ceramic membranes for oxygen separation. The kinetics of the EVD process, the morphology of the grown layers and their oxygen permeation properties are investigated. At a deposition temperature of 800°C, the EVD layer growth is limited by bulk electrochemical transport. At 1000°C the layer growth is limited by pore diffusion of the oxygen source reactant. The EVD-grown ZYT layers show columnar structures with prismatic grains on top; the size of the grains (1 to 2 μm) increases slightly with temperature and deposition time. ZYT is deposited mainly in the cubic doped zirconia phase. Oxygen permeation experiments show that the oxygen permeation flux through the ZYT layers is limited by an electrochemical process. Permeation values in the order of 10^{-8} mol/cm^2 s have been observed (900-1000°C, air *vs.* CO/CO_2).

Introduction

Yttria-stabilized zirconia (YSZ) is a well-known solid electrolyte with high ionic conductivity, high thermal and chemical stability. This material is used frequently as electrolyte phase in solid oxide fuel cells (SOFC), in oxygen sensors, and in oxygen pumps. For these purposes a low electronic conductivity is required.

To be suitable as a membrane for oxygen separation by means of an electrochemical process, both the oxygen ionic and electronic conductivity should be high. For the case of bulk YSZ its low electronic conductivity limits the electrochemical oxygen permeation. It is possible to improve the oxygen permeation by enhancing the electronic conductivity by doping YSZ with a multivalent ion, *e.g.,* titanium,[1] cerium,[2] or terbium.[3,4] The valence change of the multivalent cations results in an increased electronic conductivity due to hopping of electrons or electron holes among the multivalent cations. In this investigation terbia is chosen to enhance the electronic conductivity. The ionic conductivity should maintain its high value. Besides the use of mixed (ionic and electronic) conducting materials in oxygen separation membranes, other applications are found in electrocatalytic reactors and as cathode material for SOFC.

Oxygen permeation through a mixed conducting membrane increases when the thickness of the membrane decreases until a surface exchange reaction becomes rate-limiting for the permeation process. A suitable technique for growing thin, dense, solid oxide films (on porous substrates) is chemical/electrochemical vapor deposition (CVD/EVD). This technique was introduced by Isenberg[5] to deposit dense YSZ and Ce-doped YSZ films on porous ceramic substrates. YSZ layers with thicknesses in the range

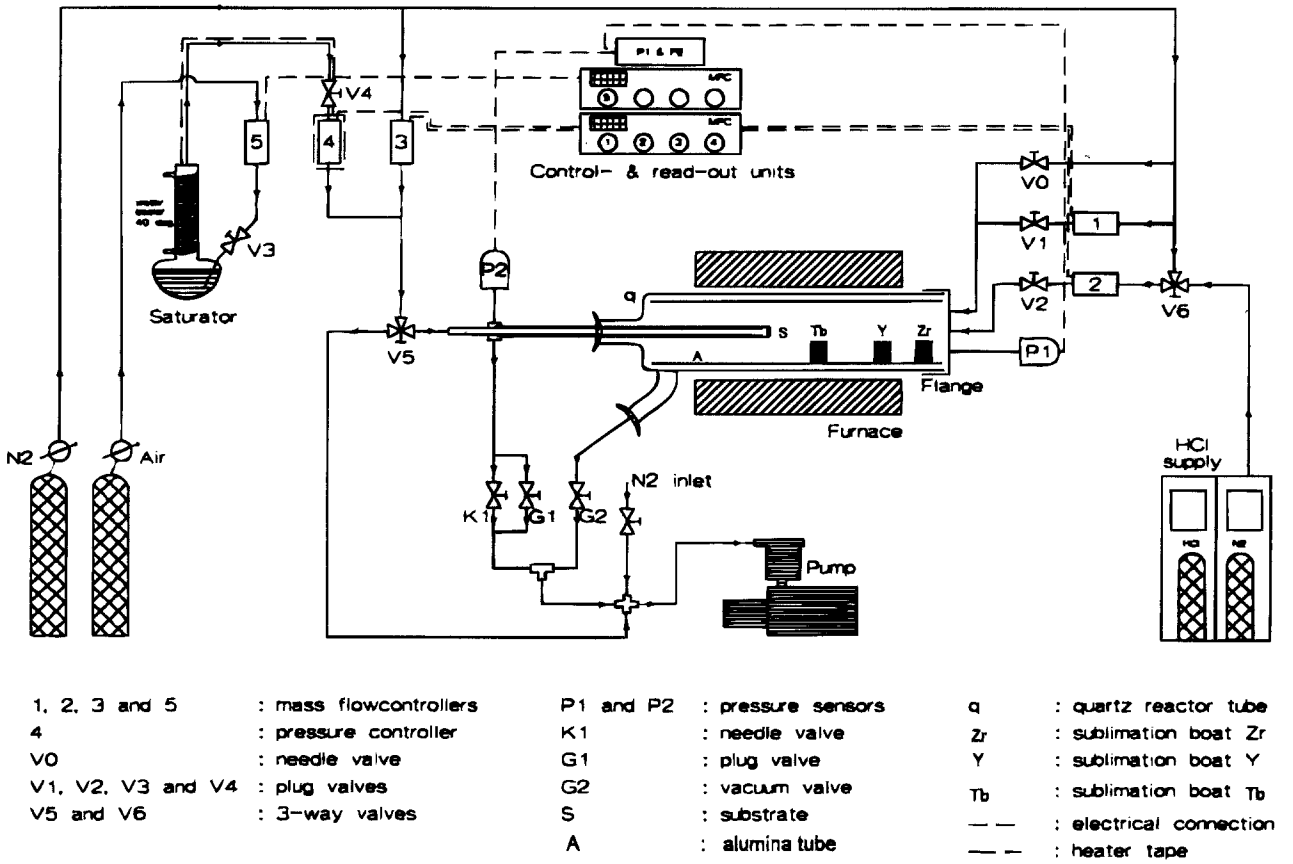

Fig. 1. Schematic overview of the MM2 equipment.

of several tenths of a micrometer to ~50 μm have been reported (see, *e.g.*, Ref. 5-8).

An extensive outline of the principles of the CVD/EVD technique for depositing solid oxides on or in porous substrates is given in Ref. 5, 8-10. The technique is briefly outlined here for completeness. A mixture of metal chloride reactants is separated from a (mixture of) oxygen containing reactants(s) by a porous ceramic substrate. Under certain process conditions the reactants diffuse into the substrate pores and react to form a metal oxide that deposits on the internal pore wall. When this process continues, pore narrowing occurs until the pores become totally blocked (plugged) with the metal oxide. Up to that point, the process is known as the opposite reactant CVD (ORCVD) process.[11,12] The process is followed by the so-called EVD process when the deposited solid oxide is mixed (oxygen ionic and electronic) conducting. A solid oxide film grows on the substrate, and the total film growth process consists of four steps: (*i*) diffusion of oxygen containing reactant(s) through the substrate pores to the plug; (*ii*) reduction of the oxygen containing reactant(s) at the oxygen source/film interface; (*iii*) migration of oxygen ions (balanced by electrons or electron holes) through the film to the film/metal chloride interface; and (*iv*) reaction at this interface of oxygen ions with the metal chlorides to form the metal oxide.

EVD of mixed conducting yttria/terbia stabilized zirconia (ZYT) on porous ceramic substrates is investigated. Kinetic, morphological, and oxygen permeation aspects are described and discussed. The influence of temperature and substrate characteristics on the ZYT layer growth rate is investigated. When electrochemical diffusion through the layer is the rate-limiting step for EVD layer growth, it is expected that layers containing the electronically conducting dopant terbia grow much faster than layers without terbia (*e.g.*, YSZ). When pore diffusion of the oxygen containing reactant(s) is rate-limiting, no difference is expected between the layer growth rate of ZYT and YSZ. Morphologic aspects are focused on the composition and distribution of zirconia, yttria, and terbia in the layers and on the relation between the average crystallite size and EVD process conditions. Oxygen permeation experiments with one EVD-formed ZYT layer was performed in an oxygen permeation reactor. A comparison is made with EVD-grown YSZ layers which are described and discussed in Ref. 13, 14.

Experimental

EVD of ZYT Layers on Porous Substrates

Description of the CVD/EVD equipment.—All CVD/EVD experiments are performed in a home-made reactor called the MM2 (membrane modifier 2). In Fig. 1 a schematic overview is given of the MM2 equipment. The central part of the equipment is a single-zone tubular furnace (Vectstar), temperature controlled by an 815P Type Eurotherm. Three dense α-alumina sublimation beds for $ZrCl_4$ powder (99.9%, 200 mesh, Cerac), YCl_3 powder (99.9%, 60 mesh, Cerac), and $TbCl_3 \cdot 6H_2O$ pellets (99.9%, Janssen Chimica) are positioned in a quartz reactor tube (q). This tube can be disconnected from the outer atmosphere to allow low pressure experiments inside the tube. It is known[15,16] that lanthanide halogenides react with quartz; to prevent this disintegration of the quartz tube, a dense α-alumina tube (A) is inserted inside the quartz tube. This metal chloride generating section is further referred to as the chloride chamber. An N_2 gas supply system and a precursor drying system [including a safety cupboard (Union Carbide) in which HCl (Praxair) was stored] are connected to this chamber. A small dense α-alumina tube (od 15 mm) with a porous ceramic substrate (S) sealed at the end is positioned in the chloride chamber. This small alumina tube is further referred to as the water chamber (WC) with a total volume of 133 ml. The oxygen-containing reactant which is delivered through this chamber to the porous substrate is a 1/1 air/water mixture in all experiments. The low pressure in the chloride chamber, water chamber, and the water saturator is maintained by a vacuum pump (Leybold Heraeus). All valves, pressures, and mass flows are con-

Table I. CVD/EVD ceramic substrate characteristics.

Substrate type	Thickness (mm)	Mean pore diameter (μm)	Porosity (%)	Fabrication method[a]
Coarse porous α-alumina[b]	2	0.16	50	Pressing, sintering
Supported La-doped γ-alumina[b]	5 μm	0.02	47	Sol-gel, dipcoating, drying, sintering
NKA α-alumina	2	1.0	43	NKA[c]
$Sr_{0.15}La_{0.85}MnO_3$ [d]	2	0.9	67	Gel casting, sintering
$(ZrO_2)_{0.92}(Y_2O_3)_{0.08}$ [d]	2	0.2	57	Gel casting, sintering

[a] All substrates except NKA α-alumina are home-made.
[b] Preparation is described in Ref. 17; the γ-alumina top layer is always faced toward the water chamber.
[c] Nederlands Keramisch Atelier.
[d] Preparation is described in internal report CT93/437/31.

trolled manually. A more extended description of the MM2 equipment is given in Ref. 14.

Deposition experiments are performed at temperatures between 800 and 1000°C. Since the furnace has only one heating zone, the positions of the metal chloride sublimation beds are dependent on the deposition temperature (temperature of the single heating zone, also known as reactor temperature). The beds are placed at specific locations in the temperature profile of the chloride chamber to obtain a sufficiently high vapor pressure for the individual metal chlorides. A nominal composition $(ZrO_2)_{0.70}(Y_2O_3)_{0.05}(Tb_2O_{3.5})_{0.25}$ is aimed at. Due to the low $TbCl_3$ vapor pressure at temperatures below 950°C, it is not possible to place the $TbCl_3$ sublimation bed in such a position that the $TbCl_3/ZrCl_4$ and $TbCl_3/YCl_3$ vapor pressure ratios are the same as at 1000°C. Below 950°C for the $TbCl_3$ bed a distance of 55 cm from the beginning of the quartz tube at the right side is chosen as a compromise between a highest possible temperature and a sufficient large distance from the substrate. This distance should be large enough for the $TbCl_3$ vapor to be mixed with the other metal chlorides and the carrier gas.

Experimental deposition procedure.—A porous substrate disk was sealed to the end of the alumina tube using a ceramic seal (Autostic CF8, Carlton Brown & Partners Ltd). Several types of substrates were used as can be seen in Table I. Before each deposition experiment, the three alumina sublimation beds were filled with $ZrCl_4$ and YCl_3 powder (from a glove box flushed with nitrogen) and $TbCl_3 \cdot 6H_2O$ pellets, and placed on the correct positions in the chloride chamber of the reactor. The reactor was then closed and both chambers were depressurized with a water jet pump to about 30 mbar. To dehydrate the hexahydrated $TbCl_3$ and to remove occasionally added water or oxygen from the $ZrCl_4$ and YCl_3, a drying procedure with HCl gas was carried out. After this procedure the water jet pump was replaced by the vacuum pump. Both reactor chambers were depressurized to 5 mbar and the temperature was raised to the desired deposition temperature between 800 and 1000°C with a maximum ramp of ~5°C/min.

Table II. Typical CVD/EVD experimental conditions for the MM2 reactor.

Deposition temperature	800-1000°C
Reactor pressure	500 Pa
$ZrCl_4$ sublimation bed temperature	180°C
YCl_3 sublimation bed temperature	580°C
$TbCl_3$ sublimation bed temperature	800-960°C [a]
N_2 carrier gas flow rate through chloride chamber	27.5 ml (STP)/min
Water saturator temperature	50°C
Water reflux cooler temperature	40°C
Air carrier gas flow rate through water saturator	0.7 ml(STP)/min
Total pressure in water saturator	15 kPa
Air/water ratio in vapor	1/1

[a] Depending on deposition temperature.

The deposition experiment started when the water/air flow was forced into the water chamber by directing valve V5 to the water chamber. Typical deposition conditions are given in Table II. After a desired deposition time (varying from 30 min to 4 h) the reaction was stopped by redirecting valve V5 forcing the water/air flow directly to the pump instead of to the water chamber. The reaction time, taken as the elapsed time between starting and stopping the experiment by switching the water supply, is considered long compared to any delayed effects at the start or stopping of the experiment. After ending the deposition experiment, the sample was checked *in situ* to be gastight as described in the section on Characterization of the deposited layers. A more extended description of the experimental deposition procedure is given in Ref. 14.

During the deposition procedure some small complications occurred. The main complication was a small air leak into the chloride chamber causing the metal chlorides to degenerate. Practically, it was not possible to make the reactor completely leak-free; this leakage problem was solved by using a large carrier gas flow through the chloride chamber; metal chlorides were refreshed faster (short resident times). Another complication, which is inherent to the ORCVD stage of the CVD/EVD process was diffusion of water from the water chamber into the chloride chamber, also causing the metal chlorides to degenerate. Also here was the remedy: a fast refreshment of the metal chlorides. Postdeposition effects (*i.e.*, continuing deposition caused by reactants still present in the substrate pores after the real deposition experiment has stopped) could be annihilated by flushing for a long time with a large nitrogen flow after the deposition experiment ceased.

Characterization of the deposited layers.—After a deposition experiment ceased an indication was given of the gastightness of the deposited sample by *in situ* nitrogen permeation. A pressure difference of 100 mbar between the chloride chamber (200 mbar) and the water chamber (100 mbar) was applied by closing the valves to the vacuum pump and flowing nitrogen into the chambers until the correct pressure was reached. The pressure in the chloride chamber was kept at 200 mbar. The total pressure (and also the pressure increase) in the water chamber was recorded every half minute for 5 min. That the water chamber had no detectable leakage was checked from the outside by closing all supplies and valves and recording the total pressure in the water chamber, which remained constant. Normal fluctuations in the pressure readout were ~0.5 mbar. If the increase in water chamber pressure after 5 min was in the order of 0.5 mbar or less, the sample was considered to be gastight.

Most of the deposited samples were investigated by x-ray diffraction (XRD, Philips PW1710 using Cu-K_α radiation with λ = 1.5418 Å) for a qualitative phase analysis. A fast line scan program was used in the range between 20 and 90°2θ. For three samples (no. 29, 38, and 60) a slow scan was recorded in the same range with scan step of 0.03°2θ and an intensity collection time of 5 s at each step. These samples were used for quantitative analysis.

Layer thickness and structure analyses were performed by scanning electron microscopy (SEM, JEOL JSM-35CF) and high resolution scanning electron microscopy (HRSEM, Hitachi S800 field emission microscope). The latter microscopic technique was used on a small selection of samples to get more detailed information at higher magnifications. SEM was used in combination with energy dispersive x-ray analysis (EDAX, KEVEX, Quantex software) for elemental analyses. Surface characteristics of the layer were analyzed by secondary electron imaging (SEI). The acceleration voltage varied between 7 and 35 keV, but the best results on these nonconductive samples were often obtained at the lower energy levels. Cross-sectional analyses

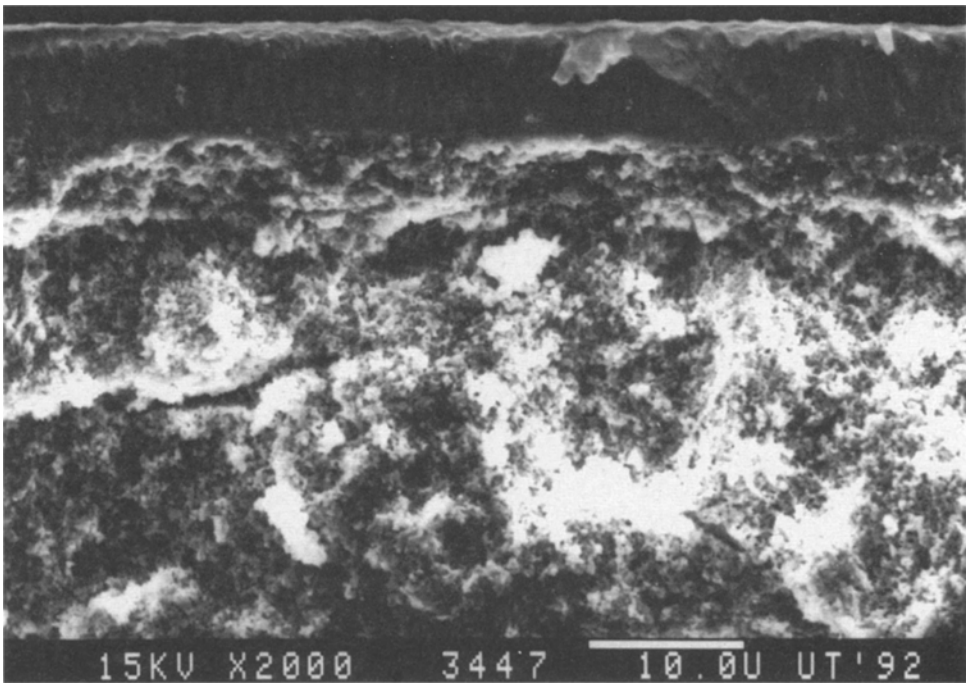

Fig. 2. SEM photograph of a cross section of an EVD-grown ZYT layer (sample 16).

were performed by SEI and BEI (backscattered electron image) separately. The ZYT layer thickness on top of the substrate material was estimated from SEI or BEI pictures on the screen. The layer thickness was measured as an average of the thickness found along the length of each sample. EDAX was performed to determine the Zr, Y, and Tb composition of the surface of the deposit (surface scan) and in the layer itself (from a cross sectioned sample). At an acceleration voltage of 35 keV K-lines were used for the elements Al, Zr, and Y; for Tb the L-line was used.

Oxygen permeation experiments.—Sample no. 76 (deposition for 3 h at 1000°C on a coarse porous α-alumina substrate, layer thickness 7-9 μm) was put in oxygen permeation reactor PR3 (of which the principles are extensively described in Ref. 18) with air (p_{O_2} = 0.21 atm) at the high and helium ($p_{O_2} \approx 10^{-4}$ atm) or a CO/CO_2 mixture ($p_{O_2} \approx 5 \cdot 10^{-16}$ atm) at the low oxygen partial pressure side. Oxygen permeation was measured at 953 and 1002°C under a large oxygen partial pressure gradient (air *vs.* CO/CO_2) and at 953°C under a small oxygen partial pressure gradient (air *vs.* He). During the measurements some leakage was observed, which became larger when measurement was attempted at 900°C.

Results and Discussion

ZYT layers grow on the side of the substrate exposed to the metal chloride vapors. At 900 and 1000°C similar columnar layer growth and crystallites on top of the surface are observed as for zirconia/yttria (see, *e.g.,* Ref. 13). At lower temperatures, *e.g.,* 800°C, no columnar structures are observed. A typical SEM photograph of a cross section of a ZYT layer deposited on a coarse porous α-alumina substrate for 125 min at 900°C (sample 16) is shown in Fig. 2. The layer has a thickness of ~7 μm. XRD analyses show that the layers formed consist mostly of the cubic doped zirconia phase; a very small amount of the monoclinic doped zirconia phase is observed.

Morphology of the deposited layers.—To get an impression of the phases formed after deposition, XRD patterns are given in Fig. 3 of three ZYT samples (deposited for 2 h at 800, 900, and 1000°C on an α-alumina substrate). The deposit consists of a fluorite-type fcc zirconia phase only, with hardly any monoclinic zirconia present. This is in contrast with EVD-grown layers of the ZrO_2-Y_2O_3 system,[13,14] in which tetragonal and/or monoclinic phases were often observed. A measurement of the amount of ZYT that has been deposited (or an indication of the ZYT layer thickness) is the ratio $I_{ct}(111)/I_{\alpha}(104)$ of the integrated K_{α_1} intensity of the cubic/tetragonal doped zirconia (111) peak around 30°2Θ and the α-alumina (104) peak around 35.1°2Θ. For samples 38, 60, and 29 (deposition for 120 min at 800, 900, and 1000°C, respectively) $I_{ct}(111)/I_{\alpha}(104)$ is 1.2, 29.3, and 53.5, respectively. At higher temperatures the ZYT layers are thicker than at lower temperatures, as is expected.

The integrated intensities for each of the ZYT peaks were compared with peak intensities of (randomly oriented) $Y_{0.15}Zr_{0.85}O_{1.93}$ powder (JCPDS card 30-1468). Preferential orientation of the ZYT layers (*i.e.*, deviation of the intensity ratios of the ZYT peaks compared to the intensity ratios of the randomly oriented powder) was hardly observed. Only at 1000°C a slight indication was given for preferential orientation since the ZYT (220) peak was somewhat higher (by a factor of 1.5) than expected for random orientation (from JCPDS card 30-1468). Preferential orientation is most likely related to the columnar layer structure that is observed, especially at higher temperatures (900 and 1000°C). Preferential orientation in the [110] direction was observed by Carolan and Michaels[20] for EVD of YSZ.

Influence of deposition parameters and substrate type on the deposit morphology.—The morphology of the surface of the ZYT top layers seems to depend on the deposition

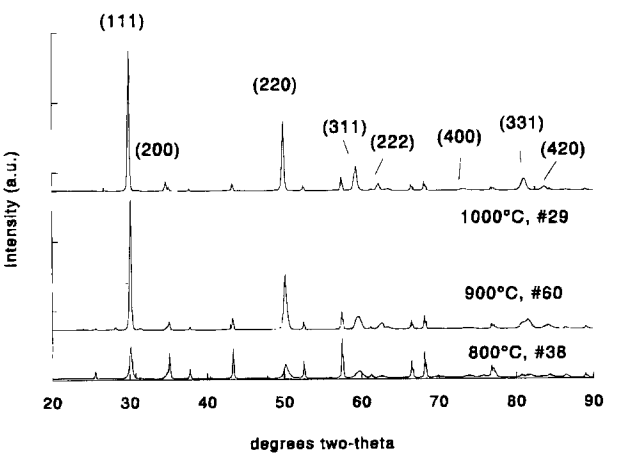

Fig. 3. XRD patterns of ZYT deposited on coarse porous α-alumina substrates for 120 min; cubic ZYT peaks are indexed.

Table III. Overview of CVD/EVD morphological aspects.

Sample no.	Substrate type[a]	T_{dep} (°C)	t_{dep} (min)	Gastight? (Y/N)	Thickness[b] (μm ± 1 μm)	Crystallite size (μm)[c]
28	α	1000	120	—	8-10	2.5
29	α	1000	120	—	5-6	1.9
30	α	1000	120	—	7-8	2.0
31	α	1000	135	—	7	—
33	α	1000	180	Y	>5	—
34	α	1000	210	Y	13	—
76	α	1000	180	Y	7-9	—
77	α	1000	120	Y	5-6	—
52	YSZ	1000	120	—	5-10	2.4
53	YSZ	1000	120	Y	3	1.5
55	NKA	1000	120	Y	4-5	3.1
51	15SLM	1000	150	—	4-30[e]	—
59	α	950	120	Y	4-6	1.4
16	α	900	125	N	—	1.5
19	α	900	240	Y	2	1
25	α	900	150	N	—	1-2
60	α	900	120	Y	5-6	3.1
57	α	850	120	Y	2-8[e]	1.5
66	α	850	120	Y	1-2[d]	—
44	α	800	60	Y	2	—
40	α	800	90	Y	1-3	—
41	α	800	90	Y	~0[d]	—
42	α	800	90	Y	0-0.5	—
37	α	800	120	—	—	—
38	α	800	120	—	1-2[e]	0.8
39	α	800	120	—	1	—
43	α	800	180	N	1-3[e]	—
48	α	800	180	Y	3-4[e]	1.1
65	α	800	240	Y	0-9	1.6
50	αγ	800	120	Y	1	0.8
67	NKA	800	120	Y	0	—
56	NKA	800	120	N	0	—

[a] α = coarse porous α-alumina, αγ = La-doped γ-alumina membrane, NKA = NKA α-alumina, YSZ = $(ZrO_2)_{0.92}(Y_2O_3)_{0.08}$, 15SLM = $Sr_{0.15}La_{0.85}MnO_3$.
[b] Determined by SEI/BEI.
[c] Determined by SEM and HRSEM.
[d] Mainly cauliflower deposit structure.
[e] Both prismatic grains and cauliflower structures.

temperature. Some morphological aspects are shown in Table III as function of deposition parameters. At high deposition temperatures (*e.g.*, 900-1000°C) EVD layers on coarse porous α-alumina, $(ZrO_2)_{0.92}(Y_2O_3)_{0.08}$ and NKA substrates exhibit a columnar structure (Fig. 2). Prismatic structures were found on top of the columns. A summary of the average sizes of the prismatic grains is presented in Table III.

At temperatures below 900°C other undesired morphologies were observed. At a deposition temperature of 850°C and a deposition time of 2 h, both prismatic and cauliflower structures were observed. At a temperature of 800°C, different surface structures of ZYT on coarse porous α-alumina were found, depending on deposition time. After 1 h deposition, the grains of the substrate were covered with a thin layer (surface modification) and the samples were not gastight. Cauliflower structures were found near the edge of the samples. When the deposition time was somewhat longer (1.5 h) cauliflower-like structures were observed at several positions on the α-alumina substrate surface, but mostly near the edge of the substrate. Some prismatic grains also could be observed. At longer deposition times (2-4 h), thin gastight layers were observed. However, cauliflower structures were found on several samples. No correlation could be observed between the deposition conditions and the morphology of ZYT layers grown on coarse porous α-alumina substrates deposited at 800°C; even under similar conditions the scatter was large.

Deposition at 800°C for 2 h on an La-doped γ-alumina membrane composite (sample 50) resulted in a 1 μm thin gastight ZYT layer on top of the γ-alumina membrane layer. The prismatic structures were smaller and rounder than those observed on any other sample.

It was not possible to obtain dense deposits of ZYT on $Sr_{0.15}La_{0.85}MnO_3$ substrates. Only homogeneous deposits which had a bad adherence to the substrate were found on top of this substrate. On a cross section of sample 51 a 3 to 5 μm thick deposition layer was found, with a homogeneous deposit on top ~30 μm thick, characterized by cauliflower structures. Deposition of ZYT on an NKA α-alumina substrate (with about the same pore size as $Sr_{0.15}La_{0.85}MnO_3$) showed a dense EVD layer of ~5 μm after 2 h of deposition at 1000°C (sample 55). The main difference between the two substrates is the substrate material. Bad adherence between the ZYT deposit and the porous $Sr_{0.15}La_{0.85}MnO_3$ substrate may be the cause for trouble with this substrate material. Also the pore size distribution of $Sr_{0.15}La_{0.85}MnO_3$ was broad; water can diffuse easily through large pores and can react at the other side of the support in the gas phase with metal chlorides. Hence a porous deposit is obtained. Deposition of ZYT on an NKA α-alumina substrate at 800°C resulted only in a surface modification, and no EVD layer was observed.

Some samples were not gastight even after a considerable deposition time. On these samples, no real EVD layers could be observed. In experiments 45-47 (deposition at 800°C for 4, 1.5, and 1 h, respectively, not shown in Table III) old $ZrCl_4$ and YCl_3 precursors, left over from earlier experiments, were used, while the $TbCl_3$ precursor was refreshed for each of these experiments. The normal drying procedure with HCl was carried out for all these samples. It is concluded that precursors should not be reused, because they cannot be regenerated to a sufficient level by normal drying procedures.

From the observations discussed above it is clear that the formation of an EVD-grown ZYT layer on coarse porous α-alumina (and other) substrates is easier at temperatures 900 ~ 1000°C than at 800°C. Deposition of ZYT at a temperature of 800°C leads to surface modification and cauliflower structures on top of the porous substrate, besides the desired prismatic layer growth. This phenomenon does not occur with deposition of zirconia/yttria layers which could be prepared at 800°C.[13,21]

Influence of deposition parameters and substrate type on the layer thickness.—The EVD-grown ZYT layer thicknesses, found by SEM and HRSEM analyses, are given in Table III as a function of deposition parameters and substrate types. This Table shows that there is a large scatter in data between samples grown under similar conditions. Especially at 800 and 850°C it is difficult to estimate the thickness of a dense EVD-grown layer. However, a clear trend in the results is obtained for the coarse porous α-alumina substrates. The ZYT layer (grown for a certain time) becomes thicker as the deposition temperature increases. At 1000°C the layer thickness is in the range of 5 to 10 μm (with an average of 7-8 μm) after 2 h deposition, decreasing to 1-2 μm at 800°C. Sample 60 showed a layer of 5 to 6 μm thickness deposited at 900°C for 2 h. This sample was accidentally left in the reactor after stopping the experiment, for more than 2 days at 900°C. This means that traces of oxygen source reactants (*e.g.*, H_2O or O_2) in the nitrogen flow through the water chamber, could have continued the reaction to some extent. For the $(ZrO_2)_{0.92}(Y_2O_3)_{0.08}$ substrate with an almost similar average pore size as coarse porous α-alumina the ZYT layer has also grown between 5 and 10 μm in 2 h. For $Sr_{0.15}La_{0.85}MnO_3$ substrates it was not possible to estimate the thickness of a dense ZYT layer.

Influence of deposition parameters and substrate type on the crystallite size.—In Table III the relation is shown between experimental conditions (*i.e.*, deposition temperature, deposition time, substrate type), layer thickness, and the average size of the crystallites observed on the surface of EVD-grown ZYT layers. It appears that when the ZYT layer is thicker (*i.e.*, at higher deposition temperature), the crystallite size increases. This has also been observed for EVD-grown zirconia/yttria layers reported in Ref. 13, 14. No clear relation is observed between substrate type and crystallite size. The average crystallite size of layers grown at 1000°C for about 2 h is around 2 μm (±0.5 μm). At this temperature the smallest prismatic structures were found on sample 58 consisting of zirconia doped with terbia only.

As an example, in Fig. 4 an HRSEM photograph is given of the top surface of an EVD-grown ZYT layer (no. 30), grown at 1000°C for 2 h on a coarse porous α-alumina substrate. Here the ZYT layer thickness is 7-8 μm, the average crystallite size is 2 μm.

At 900°C the average crystallite size is ~1.5 μm. Here the largest prismatic structures are found on sample 60, that was accidentally left at 900°C (after stopping the experiment) for about 70 h, before cooling.

The average grain size of ZYT layers grown at 800°C on coarse porous α-alumina is about 1.2 μm and increases with increasing deposition time (*i.e.*, layer thickness). Deposition at 800°C for 2 h on an La-doped γ-alumina membrane (sample 50, layer thickness 1 μm) results in small crystallites (500-800 nm).

Transmission electron microscopic (TEM) results of an EVD-grown YSZ layer (see Ref. 13, 14) revealed that the size of the crystallites was rather uniform in three dimensions; the crystallite shape was not columnar. When this is extrapolated to the results presented here, each layer (hence also each column) consists of about 2 to 4 crystallites and about a similar number of grain boundaries perpendicular to the thickness direction. A schematic representation of this microstructural feature is given in Fig. 8 of Ref. 13.

Influence of deposition parameters and substrate type on the layer composition.—Energy dispersive x-ray analyses (EDAX) were used for elemental analyses. EDAX line scans were made to obtain a composition profile. At an acceleration voltage of 35 keV Al-K, Zr-K, Y-K, and Tb-L lines were used. The accuracy of the EDAX was checked by analyzing three polished yttria-doped zirconia samples that had been analyzed by x-ray fluorescence spectroscopy (XRF). The EDAX results showed an overestimation of the amount of yttria by about 3 mole percent (m/o). Incorporating the roughness of the EVD-grown samples, the error in the compositions found by EDAX was estimated to be ~5%.

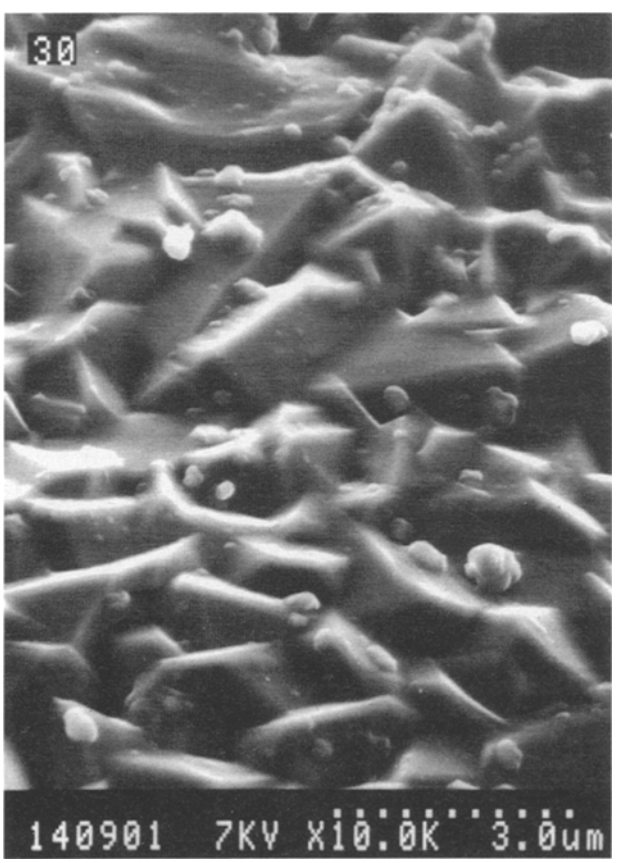

Fig. 4. HRSEM photograph of the top surface of an EVD-grown ZYT layer (sample 30), grown at 1000°C for 2 h on a coarse porous α-alumina substrate. ZYT layer thickness 7-8 μm, average crystallite size 2 μm.

Table IV. Composition of EVD-grown ZYT layers measured by EDX.

Sample no.[a]	T_{dep} (°C)	t_{dep} (min)	S(urface)/ L(ayer) scan	[Zr] [a/o]	[Y] [a/o]	[Tb] [a/o]
29	1000[d]	120	S	76	7	17
59	950	120	S	80	12	8
60	900	120	S	88	4	8
			L	86	4	10
57	850	120	S	83	3	14
66	850	120	S[b]	83	3	14
			S[c]	82	3	15
44	800[e]	60	L	89	4	7
42	800	90	L	87	6	7
38	800	120	S	92	2	6
43	800	180	L	91	2	7
			S[b]	74	5	21
			S[c]	88	4	8
65	800	240	L	88	1	11
			S	69-80	3-4	17-27

[a] All ZYT layers are deposited on a coarse porous α-alumina substrate.
[b] Scan of cauliflower structures.
[c] Scan of modified substrate.
[d] Expected vapor pressure ratio at 1000°C: $ZrCl_4$:YCl_3:$TbCl_3$ = 58.9:2.4:38.7.
[e] Expected vapor pressure ratio at 800°C: $ZrCl_4$:YCl_3:$TbCl_3$ = 92.2:3.7:4.1.

For most samples a scan was made on two or more different sites. The observed compositions of the substrate surface and inside the EVD layer (both as measured) are presented in Table IV; the presented values are averaged values of the number of sites scanned. All samples consist of more than 74 atom percent (a/o) zirconium. The amount of yttrium is not larger than 6 a/o with an exception of sample 59. According to the XRF comparison these numbers should be even lower. The amount of terbium varies between 6 and 27 a/o.

The amounts of yttrium are in good agreement with the amounts expected from the vapor pressure ratios in the metal chloride chamber (Table IV). The amounts of terbium are relatively high at 800°C (6-27 a/o) at deposition times of 3 or 4 h (samples 43 and 65, respectively), compared to what is expected from vapor pressure ratios in the metal chloride chamber. The amounts of terbium are relatively low at 1000°C (17 a/o for sample 29) compared to what is expected. However, the terbium concentration was lower than was aimed at: $(ZrO_2)_{0.70}(Y_2O_3)_{0.05}(Tb_2O_{3.5})_{0.25}$. The terbium concentrations show large variations which may be caused by the inaccuracy of the EDAX method and/or the positioning of the $TbCl_3$ sublimation bed. Incomplete mixing of $TbCl_3$ with the other metal chloride vapors and the nitrogen carrier gas may have occurred over the short distance to the substrate, especially at 800°C. The distance of the terbium chloride sublimation bed to the substrate is ~20 cm at 1000°C and ~6 cm at 800°C. The high amounts of terbium at long deposition times (samples 43 and 44) may be caused by the fact that the other chlorides degenerate faster in time by possible (practically unavoidable) oxygen leakage into the reactor. Variations in the yttria concentration can be caused by the positioning of the YCl_3 sublimation bed in that part of the reactor where a steep temperature profile exists; small variations in position cause large changes in the sublimation bed temperature.

Kinetics of EVD Growth of Zirconia/Yttria/Terbia Layers

Influence of deposition temperature and time.—Although a large scatter in layer thicknesses was found (Table III) an attempt is made to determine the growth rate constant for EVD layer growth of terbia/yttria/zirconia on coarse porous α-alumina between 800 and 1000°C. The layer thicknesses *vs.* deposition time for ZYT on α-alumina

at 800 and 1000°C are shown in Fig. 5. The straight lines through the measuring points are drawn using a least square fitting method; this does not imply, however, that a linear layer growth regime should hold for these data. The error bars are estimated from the variance in observed layer thickness by SEM.

The linear layer growth rate constant at 1000°C for ZYT on coarse porous α-alumina is 4 ± 1 μm/h according to Fig. 5, corresponding with an oxygen permeation value of about 5×10^{-9} mol/cm^2 s. When this is compared to the growth rate constant at 1000°C for the zirconia/yttria system that is described in Ref. 13, 14, the difference is about a factor 2.5 (1.6 μm/h for zirconia/yttria at 1000°C). [13,14] For the zirconia/yttria system at 1000°C and 2 mbar on a coarse porous α-alumina substrate (in another CVD/EVD reactor) the layer growth is limited by diffusion of the (water containing) oxygen source reactant through the substrate pores.[13] For the ZYT system at 1000°C and 5 mbar on a coarse porous α-alumina substrate also the pore diffusion is rate-limiting; the difference by a factor 2.5 originates because the oxygen partial pressures in the both CVD/EVD reactors under standard operating conditions differ by a factor 2.5. This is all in accordance with Eq. 2 in Ref. 13 for pore diffusion of the oxygen source reactants. From this, we conclude that the rate-limiting step for deposition of ZYT on α-alumina substrates at 1000°C and low pressure is pore diffusion of the (water containing) oxygen source reactant.

The line drawn at 800°C in Fig. 5 is based on data points with a relative large scatter; large deviations of the layer thickness were found over the substrate surface. At short deposition times only surface modifications were found. At longer deposition times the surfaces were locally covered with cauliflower structures, in most cases located only on the edge of the substrates. Only when the deposition time was 2 h or longer, dense EVD layers started to develop. More details on the morphology of the surfaces were given in section on Influence of deposition parameters and substrate type on the deposit morphology. If the experimental points in Fig. 5 are fit to a straight line the linear layer growth rate constant at 800°C is 1.2 ± 0.4 μm/h, corresponding with an oxygen permeation value of about 2×10^{-9} mol/cm^2 s. In Ref. 14, 21, for the zirconia/yttria system deposited at 800°C and 2 mbar on a coarse porous α-alumina substrate, no detectable EVD layer growth was reported between 2 and 4 h of deposition. This implies that introducing an electronic conducting component (here terbia) to the mainly ionic conducting zirconia/yttria system really increases the layer growth rate at 800°C. This has also been observed by Isenberg[5] where the addition of 5 m/o ceria increased the YSZ layer growth by a factor of nearly three.

At 800°C pore diffusion is no longer rate-limiting for ZYT layer growth. If pore diffusion should be rate-limiting at 800°C the layer growth rate should be larger than at 1000°C as is shown in Ref. 21 (see, *e.g.*, Fig. 3 in this reference).

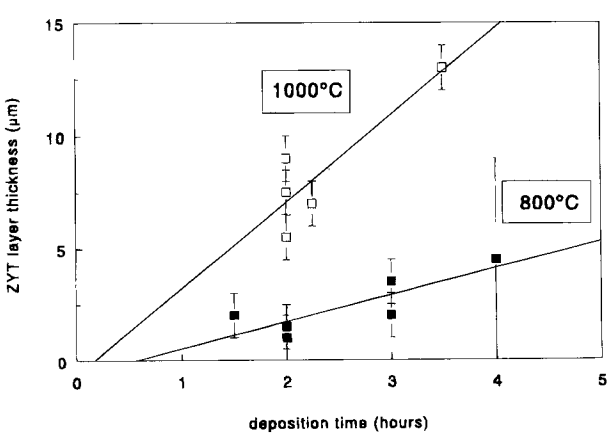

Fig. 5. ZYT layer thickness as function of deposition time at 800 and 1000°C, grown on coarse porous α-alumina substrates.

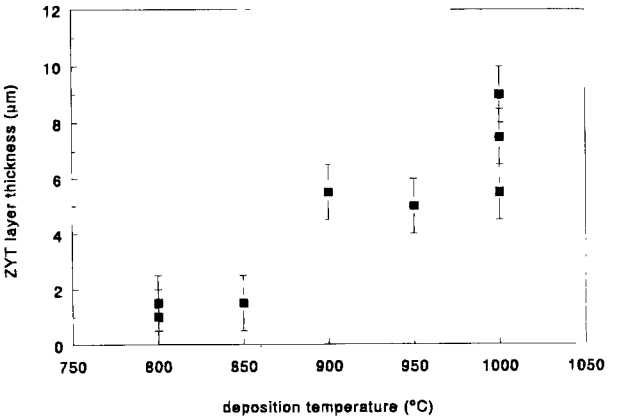

Fig. 6. ZYT layer thickness as function of deposition temperature after 2 h deposition on coarse porous α-alumina substrates.

From this, with the same arguments as in Ref. 13, 21, we conclude that the bulk electrochemical transport is rate-limiting at 800°C. For zirconia/yttria at 800°C, the electronic conductivity limits the EVD layer growth. An increased electronic conductivity by doping zirconia/yttria with Tb enhances the EVD layer growth rate at 800°C. Using the data of Fig. 5 and transforming them to the squared layer thickness *vs.* time, a parabolic growth rate constant for ZYT at 800°C is about 6 ± 2 μm^2/h, again corresponding with an oxygen permeation value of about 2×10^{-9} mol/cm^2 s.

From the relation between the ZYT layer thickness and the deposition temperature at one fixed deposition time an estimate can be made of the transition temperature for the rate-limiting step (from electrochemical diffusion at 800 to pore diffusion at 1000°C). A graphical representation of this relation is shown in Fig. 6 for a deposition time of 2 h on coarse porous α-alumina substrates at each temperature. Under electrochemical diffusion limitations the layer growth rate should increase with increasing temperature (see Eq. 3 in Ref. 13); a decrease can be expected under pore diffusion limitations (Eq. 4 in Ref. 13). Therefore, a maximum in the layer growth rate is expected at the transition temperature. In Fig. 6 no real maximum is observed between 800 and 1000°C; the scatter in data is relatively large. However, a trend can be seen in Fig. 6: layers are relatively thin after 2 h deposition at 800 and 850°C, while the layers are substantially thicker at temperatures of 900°C and higher. These data suggest that the transition temperature is somewhat above 850°C.

Influence of the substrate.—The influence of the substrate is based mainly on the mean pore diameter (and also on the pore diameter/pore length ratio) and the pore size distribution. The pore diameter varies between relatively small (0.02 μm) for the La-doped γ-alumina membrane, and relatively large (1.0 μm) for the $Sr_{0.15}La_{0.85}MnO_3$ substrate, as is shown in Table I. (In the latter substrate the pore size distribution is broad.)

In Table III the ZYT layer thickness after ~2 h deposition at 800 and 1000°C for different types of substrates is given. Thicker EVD layers are obtained at higher temperatures regardless of the substrate type. Only for the $Sr_{0.15}La_{0.85}MnO_3$ substrates no dense ZYT layers were found. As mentioned before, this is probably caused by water diffusion through the substrate pores and subsequent gas-phase reaction with the metal chlorides in the chloride chamber followed by a homogeneous deposition. Therefore it is hard to compare this substrate type with the others. At a deposition temperature of 1000°C, a decrease in the EVD layer thickness (after ~2 h deposition) with increasing pore diameter was observed. Under pore diffusion limitation, an increase of the growth rate with increasing pore diameter is expected. However, substrates with large pores (*i.e.*, NKA) should have a much larger pore closure time than substrates with small pores (*i.e.*, coarse porous α-alumina).

Therefore, when EVD layer growth rates are calculated by dividing the layer thickness by the EVD deposition time (= total deposition time minus pore closure time), the large differences should disappear. This could not be checked by us since the number of successfully deposited NKA samples was too low.

At 800°C the NKA substrate with large pores shows no detectable EVD layer after 2 h deposition, while the coarse porous α-alumina substrates show a 1 to 2 μm thick EVD layer. The parabolic growth rate is small at 800°C, while the pore closure time is slightly lower as compared to the pore closure time at 1000°C. For the NKA substrate, apparently the EVD deposition time was too short to observe any layer growth. The EVD deposition time for coarse porous α-alumina substrates and also La-doped γ-alumina membranes have been long enough to develop a thin EVD layer.

Oxygen permeation experiments.—A few experiments were performed in an oxygen permeation reactor. In this reactor oxygen permeation through sample 76 (3 h deposition of ZYT at 1000°C on a coarse porous α-alumina substrate) was measured under a well-controllable high and a low oxygen partial pressure gradient at 953 and 1002°C. Oxygen permeation fluxes of 3.5×10^{-8} (±60%) and 4×10^{-8} (±30%) mol/cm^2 s were found at 953 and 1002°C, respectively, with air ($p_{O_2} = 0.21$ atm) at the high and a CO/CO_2 mixture ($p_{O_2} \approx 5 \times 10^{-16}$ atm) at the low oxygen partial pressure side. There is no strong temperature dependence for the oxygen permeation through sample 76.

An oxygen permeation flux of around 7×10^{-10} mol/cm^2 s was found for sample 76 in the permeation reactor at 953°C with air ($p_{O_2} = 0.21$ atm) at the high and helium ($p_{O_2} \approx 10^{-4}$ atm) at the low oxygen partial pressure side. Comparing this value with 76 measured under a large p_{O_2} gradient shows that the oxygen partial pressure gradient over the membrane has a large influence on the oxygen permeation. The results of sample 76 are compared with the permeation results of zirconia/yttria sample 92001 in Ref. 13, 14 where a permeation value of around 6×10^{-11} mol/cm^2 s was found at 1100°C with air ($p_{O_2} = 0.21$ atm) at the high and helium ($p_{O_2} \approx 10^{-4}$ atm) at the low oxygen partial pressure side. It seems that doping with terbia has a large influence on the oxygen permeation process. For ZYT the permeation value is one order of magnitude larger than for zirconia/yttria while the permeation temperature for ZYT is about 150°C lower! Since oxygen permeation is enlarged by enhancing the electronic conductivity (by doping with terbia) this indicates that electrochemical diffusion through the ZYT layer may (partly) be rate-limiting for the permeation process at 953°C.

Conclusion

Thin layers of zirconia/yttria/terbia (ZYT) can be deposited on porous ceramic substrates at temperatures between 800 and 1000°C. At 800°C, the EVD layer growth is limited by bulk electrochemical transport. The parabolic growth rate constant, for EVD layer growth of ZYT on coarse porous α-alumina at 800°C, is around 6 μm^2/h. Under bulk electrochemical transport limitation, the EVD layer growth is enhanced by the addition of terbia. At 1000°C, the EVD layer growth rate is limited by pore diffusion of the oxygen source reactant. The linear growth rate constant, for EVD layer growth of ZYT on coarse porous α-alumina at 1000°C, is around 4 μm/h.

The EVD-grown ZYT layers show columnar structures with prismatic grains on top at temperatures between 800 and 1000°C. The size of the grains increases slightly with temperature and deposition time. The average prismatic grain size at 800°C is less than 1 μm and at 1000°C ~2 μm. At temperatures below 900°C also cauliflower structures, deposited by a homogeneous reaction, were found. These structures do not appear at higher temperatures and longer deposition times. XRD analyses showed that the ZYT deposits mainly consist of the cubic-doped zirconia phase. Some samples show very small amounts of monoclinic phase.

Oxygen permeation values in the order of 10^{-8} mol/cm^2 s in the temperature range 900 to 1000°C under a large oxygen partial pressure gradient (air *vs.* CO/CO_2) have been observed.

Acknowledgment

This investigation was supported by the Netherlands Foundation for Chemical Research (SON, Project No. 700-332-004) with financial aid from the Netherlands Organization for Scientific Research (NWO). J. Meijerink and J. B. van der Kooij are acknowledged for building the CVD/EVD equipment and performing CVD/EVD experiments and SEM analyses. C. M. Ophuis, J. Boeijsma, M. Smithers, and Dr. B. A. van Hassel are acknowledged for supplying several porous ceramic substrates, performing XRD experiments, operating the HRSEM equipment, and performing oxygen permeation experiments, respectively.

Manuscript submitted May 8, 1995; revised manuscript received July 25, 1995.

University of Twente assisted in meeting the publication costs of this article.

REFERENCES

1. H. Arashi and H. Naito, *Solid State Ionics,* **53-56,** 431 (1992).
2. B. Calés and J. F. Baumard, *This Journal,* **131,** 2407 (1984).
3. G. Z. Cao, X. Q. Liu, H. W. Brinkman, K. J. de Vries, and A. J. Burggraaf, in *Science and Technology of Zirconia V*, p. 576, S. P. S. Badwal, M. J. Bannister, and R. H. J. Hannink, Editors, Technomic Publishing Company, Inc., Lancaster, PA (1993).
4. W. L. Worrell, P. Han, and J. Huang, in *High Temperature Electrochemical Behaviour of Fast Ion and Mixed Conductors,* Proceedings of the 14th Risø International Symposium on Materials Science, F. W. Poulsen, J. J. Bentzen, T. Jacobsen, E. Skou, and M. J. L. Østergård, Editors, p. 461, Risø National Laboratory, Roskilde, Denmark (1993).
5. A. O. Isenberg, in *Proceedings of the Symposium on Electrode Materials and Processes for Energy Conversion and Storage,* J. D. E. McIntyre, S. Srinivasan, and F. G. Will, Editors, PV 77-6, p. 572, The Electrochemical Society Proceedings Series, Princeton, NJ (1977).
6. M. F. Carolan and J. N. Michaels, *Solid State Ionics,* **37,** 189 (1990).
7. Y. S. Lin, K. J. de Vries, H. W. Brinkman, and A. J. Burggraaf, *J. Membrane Sci.,* **66,** 211 (1992).
8. G. Dietrich and W. Schäfer, *Int. J. Hydrogen Energy,* **9,** 747 (1984).
9. M. F. Carolan and J. N. Michaels, *Solid State Ionics,* **25,** 207 (1987).
10. L. G. J. de Haart, Y. S. Lin, K. J. de Vries, and A. J. Burggraaf, *J. Eur. Ceram. Soc.,* **8,** 59 (1991).
11. G. Z. Cao, H. W. Brinkman, J. Meijerink, K. J. de Vries, and A. J. Burggraaf, *J. Am. Ceram. Soc.,* **76,** 2201 (1993).
12. H. W. Brinkman, G. Z. Cao, J. Meijerink, K. J. de Vries, and A. J. Burggraaf, *Solid State Ionics,* **63-65,** 37 (1993).
13. H. W. Brinkman, J. Meijerink, K. J. de Vries, and A. J. Burggraaf, *J. Eur. Ceram. Soc.,* Accepted.
14. H. W. Brinkman, Ph.D. Thesis, University of Twente, Enschede, The Netherlands (1994).
15. M. Yamane and M. Suenaga, *J. Appl. Phys.,* **54,** 107 (1983).
16. W. van Erk and T. Rietveld, *Philips J. Res.,* **42,** 102 (1987).
17. Y. S. Lin and A. J. Burggraaf, *J. Am. Ceram. Soc.,* **74,** 219 (1991).
18. B. A. van Hassel, J. E. ten Elshof, and H. J. M. Bouwmeester, *Appl. Catal. A,* **119,** 279 (1994).
19. H. W. Brinkman, G. Z. Cao, J. Meijerink, K. J. de Vries, and A. J. Burggraaf, in *Science and Technology of Zirconia V,* S. P. S. Badwal, M. J. Bannister, and R. H. J. Hannink, Editors, p. 811, Technomic Publishing Company, Inc., Lancaster, PA (1993).
20. M. F. Carolan and J. N. Michaels, *Solid State Ionics,* **37,** 197 (1990).
21. H. W. Brinkman, G. Z. Cao, J. Meijerink, K. J. de Vries, and A. J. Burggraaf, *J. Phys. IV Colloq. C3,* **3,** 59 (1993).